MULTIPLICITY DISTRIBUTIONS IN PROTON-PROTON COLLISIONS

By A. Wróblewski

Institute of Experimental Physics, University of Warsaw*

(Presented at the XIII Cracow School of Theoretical Physics, Zakopane, June 1–12, 1973)

General features of the multiplicity distributions in proton-proton collisions are critically analysed.

1. Introduction

One of the easiest experiments to perform using bubble chamber or other technique is to study the distribution of the number of charged particles produced in inelastic collisions. New experimental results on charged multiplicities in proton-proton collisions in the range from 50 to 300 GeV/c have recently been reported and the subject has become quite fashionable to discuss.

In this paper I am going to give a review of experimental results and empirical formulae and models. I shall also present some new results of my own which have not yet been published in a written form[1].

2. Experimental data

I shall discuss available data on charged multiplicity distribution in proton-proton collisions in the range from 3.7 to 303 GeV/c [1].

It is convenient to use the probability P of producing a given number of charged prongs in an inelastic collision:

$$P_n = \frac{\sigma_n}{\sigma_{\text{inel}}} = \frac{\sigma_n}{\sum\limits_n \sigma_n}, \tag{1}$$

* Address: Instytut Fizyki Doświadczalnej, Uniwersytet Warszawski, Hoża 69, 00-681 Warszawa, Poland.

[1] The results on the skewness (Section 3), the integrated correlation functions (Section 4) and the criticism of an early semi-inclusive scaling idea (Section 6) have been first reported in lectures that I delivered in Aachen, Bonn, Hamburg, Heidelberg and Munich in December 1972. The modification of Buras-Koba scaling (Section 8) has been first reported in my lectures at the universities in Stockholm and Lund in April 1973.

where σ_n is the topologic cross-section for n-prong events and σ_{inel} is the total inelastic cross-section. Fig. 1 shows P_n as a function of the average charged multiplicity $\langle n \rangle$

$$\langle n \rangle = \frac{\sum_n n\sigma_n}{\sum_n \sigma_n} . \tag{2}$$

The lines following the values of P_n for each n have been drawn by hand only to show that there exists some regularity in the multiplicity distribution.

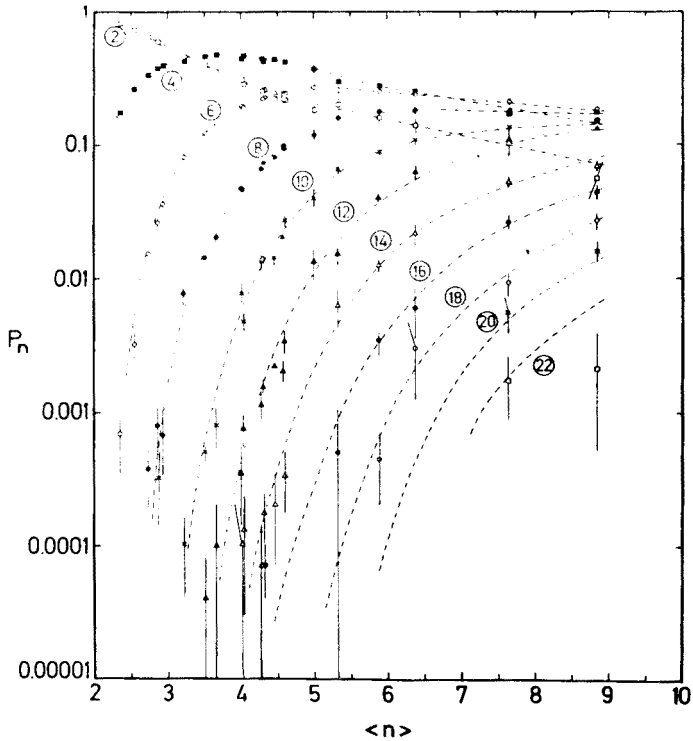

Fig. 1. The probability P_n for producing n charged prongs as a function of the average charged multiplicity $\langle n \rangle$

It is worth noticing that some large statistics experiments in the range between 12 and 28 GeV/c (corresponding to $\langle n \rangle$ between 3.5 and 4.5) recorded P_n's below 10^{-4}, whereas small statistics "pilot" experiments performed at NAL went down only to $P_n \approx 10^{-3}$, thus losing a large n tail of the distribution ($P_n \approx 5 \cdot 10^{-5}$ should correspond roughly to 34-prong events). That is an important point because the average multiplicity $\langle n \rangle$ and many other characteristic parameters of the distribution are rather sensitive to P_n's for multiplicities which are far from the average.

Another point concerns the cross-sections for inelastic two-prong events. The two-prong sample is subject to the largest scanning loses and it has then to be corrected for

elastic scattering events. The resulting sample of two-prong inelastic events may be systematically biased. Since topologic cross-sections are obtained by normalizing the total number of events to the total inelastic cross-section, the possible systematic errors in P_2 influence also the probabilities P_n for $n > 2$. This point is illustrated in Fig. 2 which shows a compilation of inelastic two-prong events in pp collisions. The large spread of points at similar energies is then reflected in the spread of parameters describing multiplicity distribution

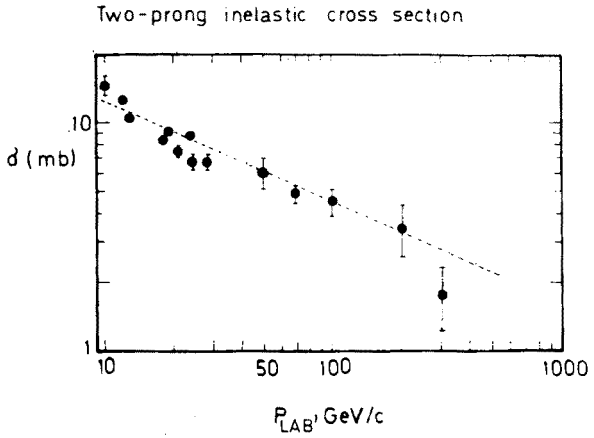

Fig. 2. Cross-section for inelastic two-prong events in proton-proton collisions. The straight line has been drawn by eye

(see Section 3). It seems also that the inelastic two-prong cross-section at 303 GeV/c is abnormally low (by $\sim$ 1 mb) compared to values at lower momenta. This point will be discussed further in Section 3.

3. Parameters of the multiplicity distribution

Let us list various parameters describing the multiplicity distribution:

1. Mean charged multiplicity $\langle n \rangle$, defined already by (2).
2. Central moments of the distribution

$$\mu_k = \langle (n - \langle n \rangle)^k \rangle. \tag{3}$$

3. Absolute moments

$$\mu'_k = \langle n^k \rangle. \tag{4}$$

4. Absolute moments can also be represented by the parameters

$$C_k = \frac{\langle n^k \rangle}{\langle n \rangle^k}. \tag{5}$$

The following parameters are of special interest:

5. The width of the distribution defined by the square root of the second central moment, or the dispersion

$$D = (\langle n^2 \rangle - \langle n \rangle^2)^{1/2} = (\mu_2)^{1/2}. \tag{6}$$

6. The asymmetry of the distribution as measured by the skewness

$$\gamma_1 = \frac{\mu_3}{D^3}. \tag{7}$$

7. The kurtosis of the distribution

$$\gamma_2 = \frac{\mu_4}{D^4}. \tag{8}$$

As mentioned before, the moments of the distribution and related parameters are sensitive to the low and high multiplicity tails. It is then reasonable [2] to use also quantities depending mostly on cross-sections for typical inelastic events which are best determined experimentally. These are:

8. The median multiplicity M_d, defined by the equation

$$\sum_{n<M_d} P_n = \sum_{n>M_d} P_n = 0.5 \tag{9}$$

and

9. The modal multiplicity, M_0, which gives the position of the peak (or mode) of the multiplicity distribution

$$\frac{d}{dn}\psi(n)\Big|_{n=M_0} = 0, \tag{10}$$

where $\psi(n)$ is the function describing the multiplicity distribution.

The dispersion of the proton-proton multiplicity distribution has been found to depend linearly on the average charged multiplicity [3]. Experimental data in the range from 4 to 303 GeV/c are well described by the formula:

$$D = A\langle n \rangle - \mathrm{B}, \tag{11}$$

where the coefficients A and B are equal within errors. The best fit to the formula

$$D = A(\langle n \rangle - 1) \tag{11a}$$

gives $A = 0.576 \pm 0.008$, so that $A^2 \approx 1/3$. These results are illustrated in Figs 3 and 4. As it has been mentioned before, significant spread of experimental points is due to systematic errors in cross-sections for two-prong inelastic events.

The skewness of the proton-proton multiplicity distribution appears to be constant in the range from 12 to 303 GeV/c (see Fig. 5):

$$\gamma_1 \approx 2/3. \tag{12}$$

Also the kurtosis γ_2 seems to have a constant value of about 3.2 in the same range of momentum, but in this case experimental uncertainties are much larger.

Making use of (11a) and (12) one can easily obtain expressions for the frequently used quantities $\langle n\rangle/D$, C_2 and C_3:

$$\frac{\langle n\rangle}{D} = \frac{1}{A}\,\frac{\langle n\rangle}{\langle n\rangle - 1}, \tag{13}$$

$$C_2 = \frac{\langle n^2\rangle}{\langle n\rangle^2} = A^2 + 1 - 2A^2\,\frac{1}{\langle n\rangle} + \frac{A^2}{\langle n\rangle^2}, \tag{14}$$

$$C_3 = \frac{\langle n^3\rangle}{\langle n\rangle^3} = \gamma_1(C_2-1)^{3/2} + 3C_2 - 2. \tag{15}$$

These quantities are plotted in Figs 6, 7 and 8. If (11a) and (12) is true also at higher energies then:

$$\frac{\langle n\rangle}{D} \to 1.732, \tag{13a}$$

$$C_2 \to 1.333, \tag{14a}$$

$$C_3 \to 2.128, \tag{15a}$$

for $\langle n\rangle \to \infty$.

It has been suggested by Slattery [4] that the normalized moments C_2 and C_3 have already reached their asymptotic limits in the range from 50 to 303 GeV/c. In my opinion

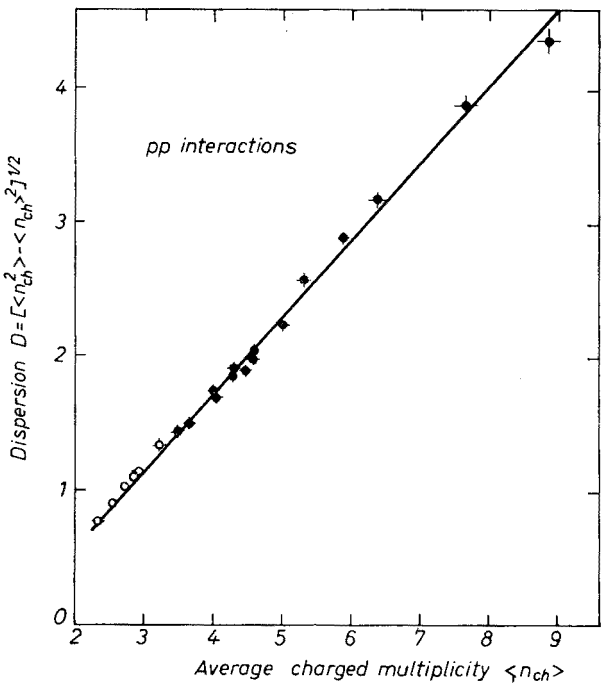

Fig. 3. Dispersion D as a function of $\langle n\rangle$. Empty circles in this and other figures show low energy data not corrected for strange particles

the experimental evidence for this conjecture is rather weak, because it is based almost only on the 303 GeV/c point. At this energy the reported two-prong cross-section is abnormally low, which results in rather low values of C_2 and C_3. If one increases the questionable cross-section by 1.2 mb from 1.8 to 3 mb (compatible with the results at lower energies) one obtains the values of C_2 and C_3 as indicated by crosses in Figs 7 and 8, and Slattery's conjecture loses support.

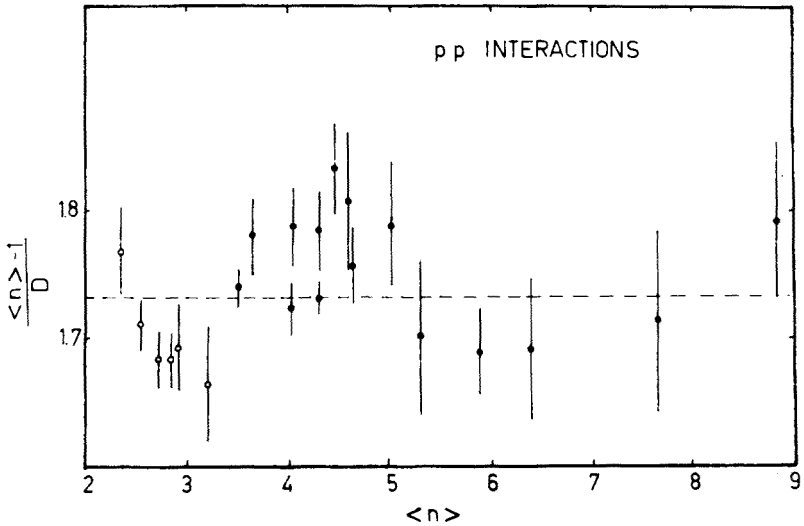

Fig. 4. The ratio of $(\langle n\rangle - 1)$ to D for pp collisions. Broken line shows the value $A = (\sqrt{3})^{-1}$

It is not my intention to correct other people's experiment. I should like only to point out the importance of two-prong inelastic cross-section which is the most difficult to determine experimentally [2].

4. *Integrated correlation functions*

The two-particle correlation function is usually defined as follows

$$C(y_1, y_2) = \frac{1}{\sigma}\frac{d^2\sigma}{dy_1 dy_2} - \frac{1}{\sigma^2}\frac{d\sigma}{dy_1}\frac{d\sigma}{dy_2}, \tag{16}$$

where σ is the total inelastic cross-section. Integrating (16) over the whole range of rapidities y_1, y_2 we obtain

$$f_2 = \int C(y_1, y_2)\, dy_1 dy_2 = \langle n(n-1)\rangle - \langle n\rangle^2, \tag{17}$$

[2] In his calculation Slattery [4] has made use of the preliminary results of the 50 GeV/c experiment as reported at the Batavia Conference. The two-prong inelastic cross-section at this energy has been since then corrected down by 0.43 mb [1]; this decreased the values of C_2 and C_3. Figs 7 and 8 show values calculated from the published data [1].

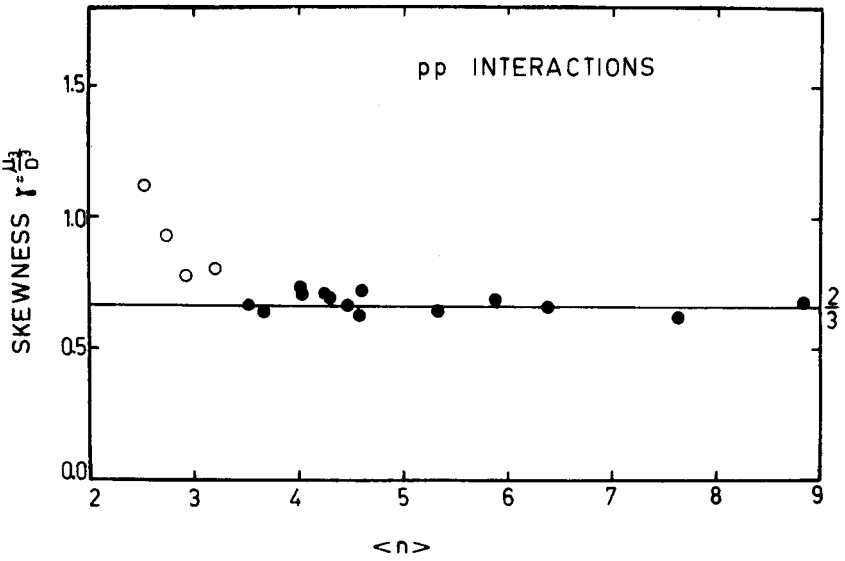

Fig. 5. The skewness γ_1 of charged multiplicity distribution for pp collisions

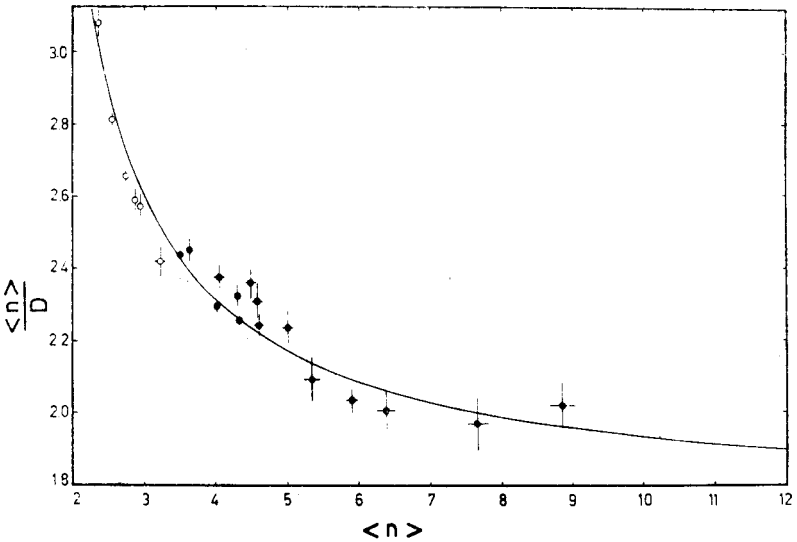

Fig. 6. The ratio $\langle n \rangle / D$ for pp collisions. The continuous line shows the prediction based on formula (13)

because

$$\int \frac{d\sigma}{dy}\, dy = \langle n \rangle \sigma \quad \text{and} \quad \int \frac{d^2\sigma}{dy_1 dy_2}\, dy_1 dy_2 = \langle n(n-1) \rangle \cdot \sigma.$$

Formula (17) can also be rewritten, using (6), in the form

$$f_2 = D^2 - \langle n \rangle. \tag{17a}$$

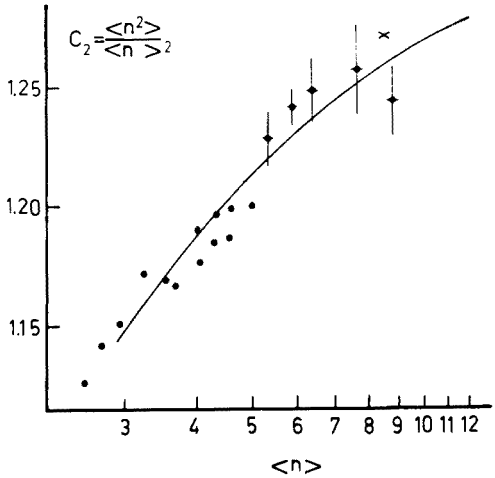

Fig. 7. Second normalized moment C_2 for pp collisions. The continuous line has been calculated according to formula (14). The cross shows the "corrected" point at 303 GeV/c (see text)

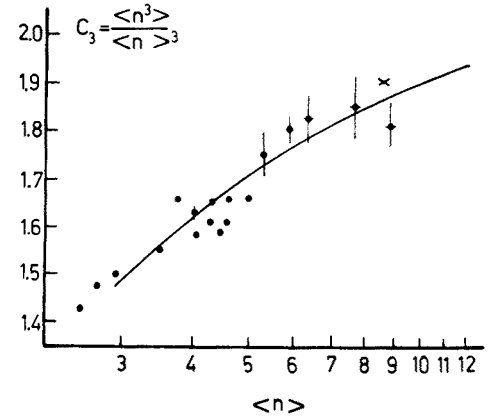

Fig. 8. Third normalized moment C_3 for pp collisions. The continuous line has been calculated according to formula (15). The cross shows the "corrected" point at 303 GeV/c (see text)

We find therefore that the integrated two-particle correlation function f_2 is determined by the parameters of multiplicity distribution. It is also easy to obtain the formula

$$f_3 = \int C(y_1, y_2, y_3)dy_1dy_2dy_3 =$$
$$= \langle n(n-1)(n-2)\rangle - 3\langle n(n-1)\rangle\langle n\rangle + 2\langle n\rangle^3 = \mu_3 + 2\langle n\rangle - 3D^2. \tag{18}$$

Let us now consider the correlation functions for negative secondary particles in pp collisions. We have

$$n_- = \tfrac{1}{2}(n-2) \tag{19}$$

and (11a) is to be rewritten as

$$D_- = A(\langle n_-\rangle + \tfrac{1}{2}). \tag{20}$$

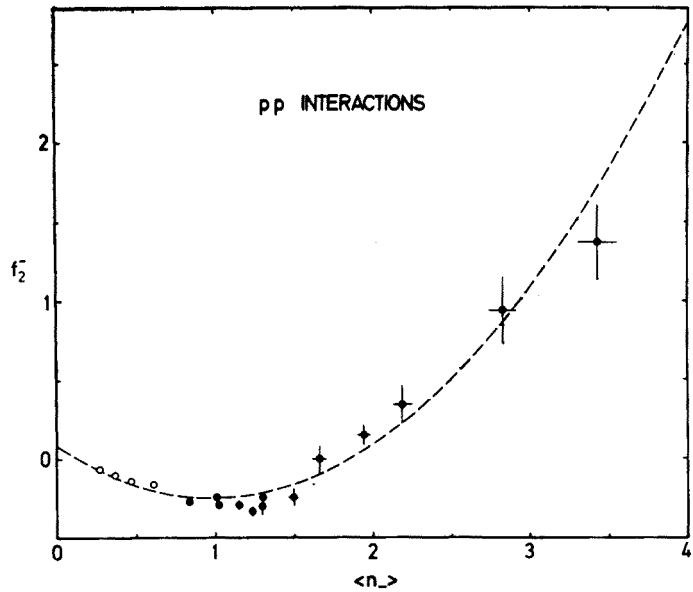

Fig. 9. Integrated two-particle correlation function f_2 for negative particles in pp collisions. The dashed line has been calculated from formula (21)

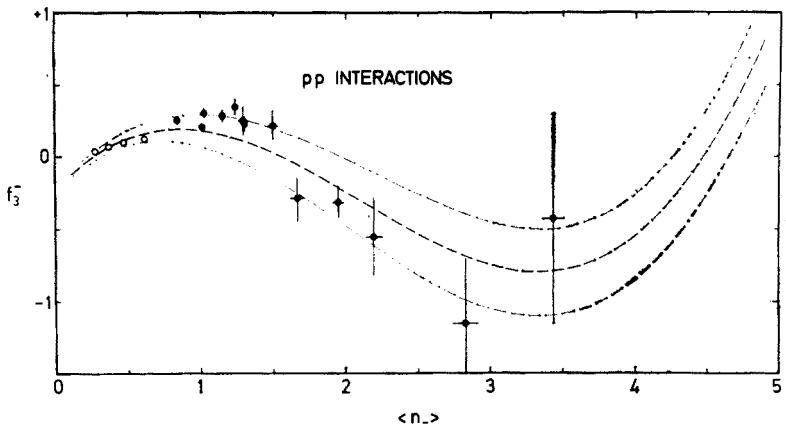

Fig. 10. Integrated three-particle correlation function f_3 for negative particles in pp collisions. The dashed line has been calculated from formula (22)

Taking $A^2 = \frac{1}{8}$ we obtain from (17a) and (20):

$$f_2^- = D_-^2 - \langle n_- \rangle = \tfrac{1}{3}\langle n_- \rangle^2 - \tfrac{2}{3}\langle n \rangle + \tfrac{1}{12}. \tag{21}$$

In a similar way we obtain an expression for f_3^-:

$$\gamma_1 = \gamma_1^- = \frac{\mu_3^-}{D_-^3} = \frac{f_3^- + 3D_-^2 - 2\langle n_- \rangle}{D_-^3} = \frac{2}{3},$$

$$f_3^- = 0.128\langle n_- \rangle^3 - 0.808\langle n_- \rangle^2 + 1.096\langle n_- \rangle - 0.234, \tag{22}$$

where we used (11a), (20) and (12). Results (21) and (22) are shown in Figs 9 and 10. The corridor of errors drawn in Fig. 10 was calculated taking 0.01 and 0.02 as the errors of A and γ_1, respectively. We see that the leading term in (22) is positive, so that if (11a) and (12) are true also at higher energies, the correlation function f_3^- will become positive near $\langle n_- \rangle \approx 4.5$, which corresponds to $p_{\mathrm{LAB}} \approx 800$ GeV/c.

5. *Empirical formulae*

For some time the Poisson distribution has been the most popular candidate for describing the charged multiplicity distribution. It has been shown [3] however, that none of existing models, which incorporate the Poisson formula, can reproduce the experimental linear dependence of D on $\langle n \rangle$. The coincidence of model prediction with experimental data at some value of $\langle n \rangle$ is purely accidental.

We shall now discuss some other empirical formulae which have been proposed during the last years.

(A) Czyżewski and Rybicki [5] have generalized the Poisson formula for non-integer variables by replacing a factorial by a Γ-function and introducing one free parameter. Their formula reads

$$P_n = \frac{d^{2\left(d\frac{n}{D} - d\frac{\langle n \rangle}{D} + d^2\right)}}{\Gamma\left(d\frac{n}{D} - d\frac{\langle n \rangle}{D} + d^2 + 1\right)} \frac{2d}{D} \exp(-d^2), \tag{23}$$

where $\langle n \rangle$ and D are taken from the experiment and d is the only parameter to be fitted. Using new variables

$$x = \frac{n - \langle n \rangle}{D}, \qquad y = D \cdot P_n, \tag{24}$$

we obtain

$$y = \frac{2d^{2(h-1)}}{\Gamma(h)} \exp(-d^2), \tag{25}$$

where $h = dx + d^2 + 1$. The formula of Czyżewski and Rybicki with $d =$ constant gives a good fit to all experimental data for pp, πp and Kp interactions (see Fig. 11) for $p_{\mathrm{LAB}} \lesssim$ $\lesssim 30$ GeV/c. It appears that the formula (25) is not very sensitive to the value of d. In Fig. 11 the curve is plotted for $d = 2$. (The best fit value of d is 1.7 for pp interactions and 2.2 for πp interactions.)

The recent pp data from Serpukhov and Batavia make it possible to check the Czyżewski-Rybicki formula for $p_{\mathrm{LAB}} \geqslant 50$ GeV/c. Fig. 12 shows the ratio R of P_n (experimental) to the probability P_n (theoretical) calculated from the formula. Instead of random fluctuations of points around $R = 1$, the data seem to show some systematic behaviour around the position of the average charged multiplicity. Assuming that the deviations from $R = 1$ depend on $n - \langle n \rangle$, the distance from the average value, one may plot in one

graph all the data for 50 GeV/$c \leqslant p_{\mathrm{LAB}} \leqslant$ 303 GeV/c, as shown in Fig. 13. Fig. 14 shows the result of combining the points into groups of five what reduces the errors and allows us to see better the systematic deviations from the Czyżewski-Rybicki formula.

One has, however, to remember that the largest systematic deviations occur at the wings of the multiplicity distribution which contain few events, so that the χ^2 values for individual experiments are still reasonable. It appears that the Czyżewski-Rybicki formula

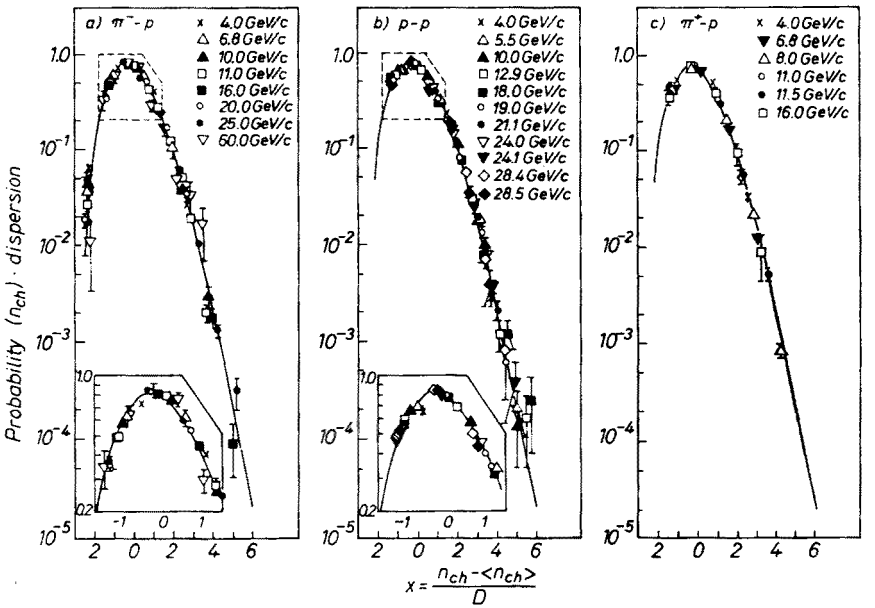

Fig. 11. Low energy data for charged multiplicity distributions fitted with the Czyżewski–Rybicki formula (from Ref. [5])

with $d =$ constant gives wrong prediction as to the position of the mode M_0, as illustrated in Fig. 15. In order to get a better fit one has to decrease d as p_{LAB} increases. At 303 GeV/c one gets for $d \approx 1.2$ a good fit and a correct position of the mode.

(B) Tati and Yokoyama [6] have introduced a scaling parameter which transforms a given distribution into a Poisson one. They define

$$n'_- = \frac{1}{\alpha_-} n_- \tag{26}$$

and assume that using n'_- one gets a Poisson distribution, so that

$$\langle n'_-(n'_- - 1)\rangle - \langle n'_-\rangle^2 = 0. \tag{27}$$

Then

$$f_2^- = (\alpha_- - 1)\langle n_-\rangle$$

or

$$\alpha_- = 1 + \frac{f_2^-}{\langle n_-\rangle} \tag{28}$$

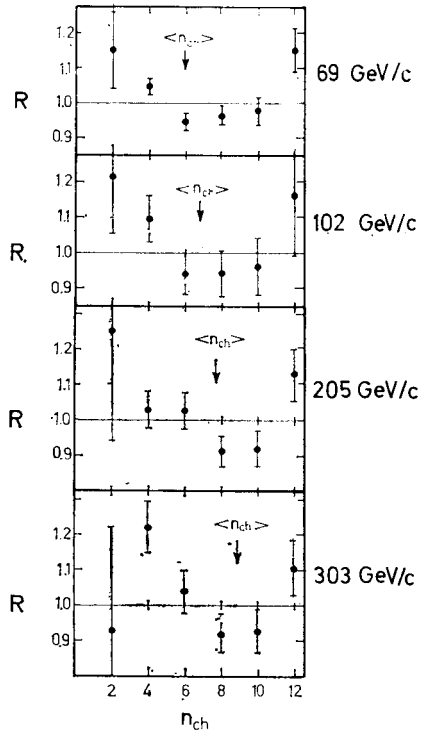

Fig. 12. Ratio R of the experimental probability P_n of producing n charged prongs to the probability calculated from the Czyżewski-Rybicki formula

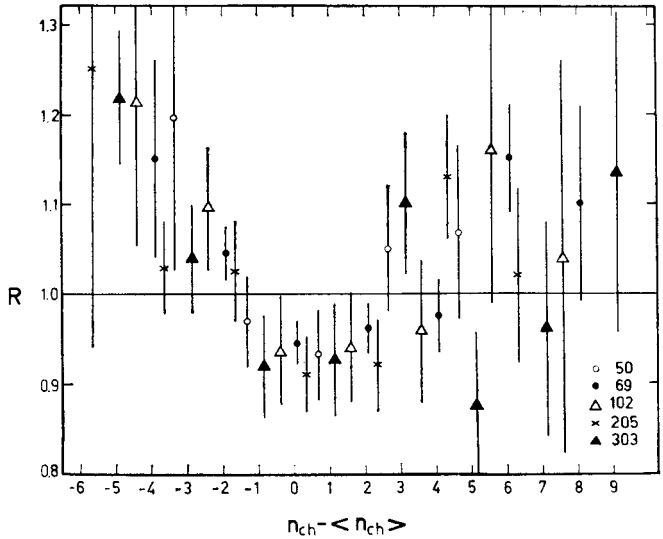

Fig. 13. Ratio R (see Fig. 12) as a function of $n - \langle n \rangle$. Experimental data are from the range 50 GeV/c $\leqslant$ $\leqslant p_{\mathrm{LAB}} \leqslant$ 303 GeV/c

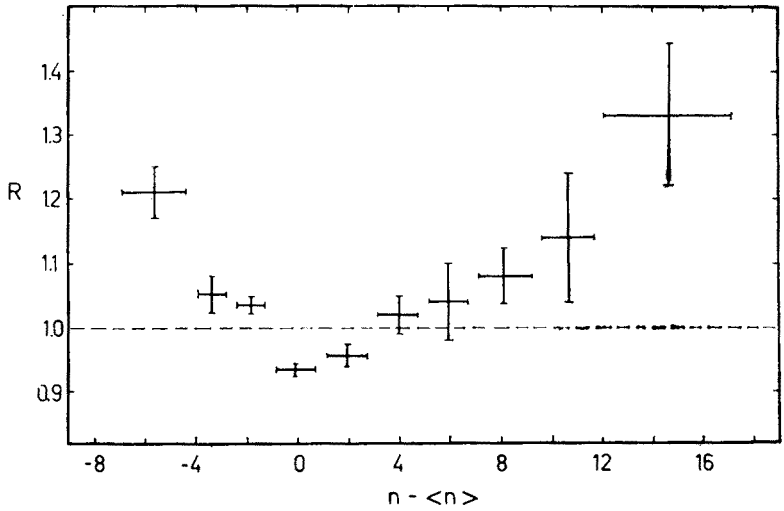

Fig. 14. Ratio R as a function of $n-\langle n\rangle$. Experimental points combined into groups of five

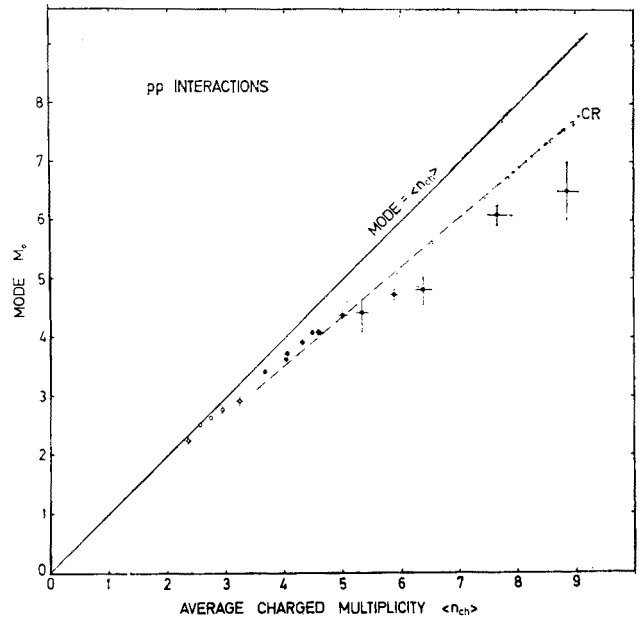

Fig. 15. Mode M_0 as a function of $\langle n\rangle$ for pp collisions. The dashed line (CR) has been calculated from the Czyżewski-Rybicki formula with $d = 1.7$. The decrease in d decreases the slope of the dashed line

and further

$$f_3^- = (\alpha_- - 1)(\alpha_- - 2)\langle n_-\rangle,$$

$$f_4^- = (\alpha_- - 1)(\alpha_- - 2)(\alpha_- - 3)\langle n\rangle, \text{ etc.} \tag{29}$$

This is an elegant representation of multiplicity distribution. However the scaling para-

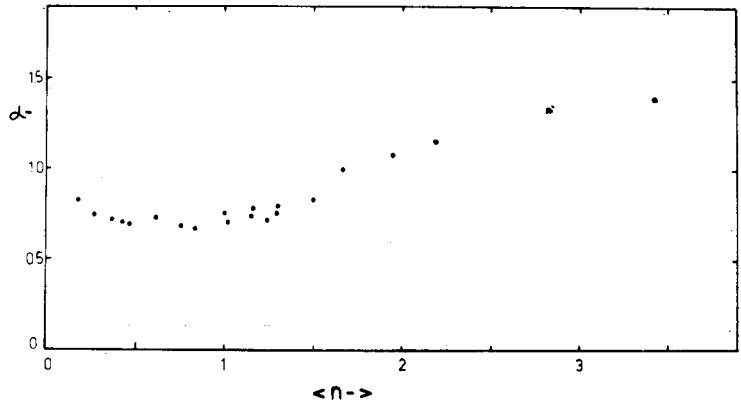

Fig. 16. Scaling parameter α_- of Tati and Yokoyama plotted as a function of $\langle n_- \rangle$

meter α_- is changing with energy in a rather erratic way, so that it is difficult to predict its behaviour at higher energies. If one assumes that at high energy α_- grows linearly with $\langle n_- \rangle$ one obtains simple predictions for integrated correlation functions [7]. It is however seen in Fig. 16 that the linear approximation for $\langle n_- \rangle > 1$ is not very good.

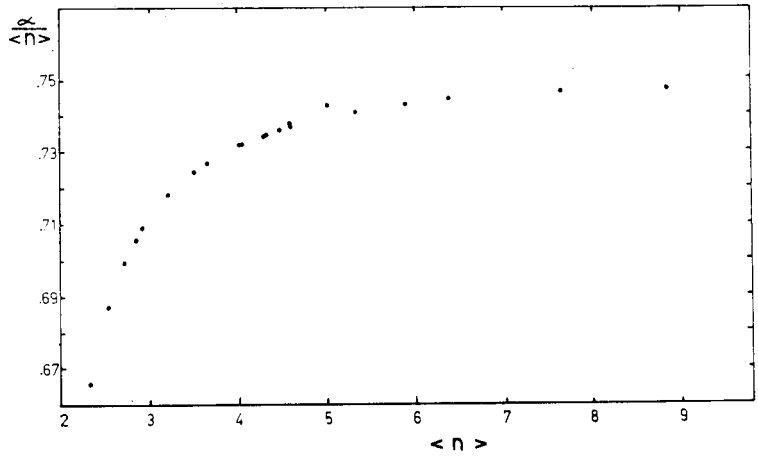

Fig. 17. The ratio $\alpha/\langle n \rangle$ for $\beta = 2.215$ in Bozoki *et al.* formula

(C) Hoang [8] has also proposed to modify the Poisson distribution by introducing a compound distribution

$$P_n = P'_n(\alpha)\,(1+\beta n)^n, \tag{30}$$

where $P'_n(\alpha)$ is an ordinary Poisson distribution with an average α. Hoang's formula thus contains two parameters to be fitted at each energy.

(D) Bozoki *et al.* [9] have proposed an empirical formula

$$P_n = c \cdot n^{\beta - 1} \exp\left(-\frac{n^2}{2\alpha^2}\right), \tag{31}$$

where c is a normalization constant determined by the condition $\sum_n P_n = 1$, and α, β are two free parameters to be fitted at each energy. The authors of Ref. [9] have obtained good fits to the data below 30 GeV/c, the data used were however of rather poor quality.

Recently Weisberg [10] used the Bozoki *et al.* formula to fit high energy data above 50 GeV/c. He has determined

$$\beta = 2.215 \pm 0.015 \ . \tag{32}$$

by fitting the normalized moments C_q and remarked that the further normalization condition

$$\sum_n n P_n = \langle n \rangle \tag{33}$$

determines then α as a function of $\langle n \rangle$. For $p_{\mathrm{LAB}} \geqslant 50$ GeV/c $\alpha/\langle n \rangle$ is indeed almost constant and (31) becomes an one-parameter formula (see Fig. 17). However at lower energies formula (31) with $\beta = \text{const.}$ as given by (32) and α determined by (33) gives poor fits to the data. In order to obtain better fits one is forced to allow both α and β to vary, so that (31) is a two-parameter formula. Weisberg's conjecture (32) can be criticised on the same grounds as the one of Slattery (see Section 3).

(E) Parry and Rotelli [11] have proposed a truncated Gaussian formula

$$P_x = \sqrt{\frac{2}{\pi}} \frac{1}{\sigma\left[1 + \Phi\left(\frac{a-2}{\sigma\sqrt{2}}\right)\right]} \exp\left[-\frac{(x-a)^2}{2\sigma^2}\right], \tag{34}$$

where

$$\Phi(z) = \frac{2}{\sqrt{\pi}} \int_0^z dt \exp\left[-t^2\right]. \tag{35}$$

In the case of usual Gaussian formula the continuous variable x runs from $-\infty$ to $+\infty$, whereas for pp interactions $x = n$ is always $\geqslant 2$, hence the reason to introduce a truncated Gaussian in which x runs from 2 to $+\infty$. Then (34) is a two-parameter formula with a and σ to be fitted at each energy. For example $a = 1.75$, $\sigma = 2.81$ at 19 GeV/c and $a = 7.0$, $\sigma = 5.64$ at 303 GeV/c. The fits are good. It is not easy, however, to extrapolate a and σ to higher energies and to predict the multiplicity distribution.

Concluding this section we find that many one- and two-parameter empirical formulae can provide reasonable fits to the experimental data. We have to await more accurate data, especially in the range above 50 GeV/c, to be able to make a proper choice.

6. *Semi-inclusive scaling (KNO scaling)*

Starting with the Feynman scaling assumption Koba, Nielsen and Olesen [12] have shown that one can obtain the following asymptotic result

$$\langle n\rangle \cdot P_n \xrightarrow[s\to\infty]{} \psi\left(\frac{n}{\langle n\rangle}\right), \tag{36}$$

where ψ is an energy independent function; its shape is not determined by theoretical arguments and is to be found from the experiment.

Slattery [4] has examined the data in the 50–300 GeV/c range and found out that the plots of $\langle n\rangle \cdot P_n$ *vs* $z = n/\langle n\rangle$ are indeed very well represented by a single curve (see Fig. 18).

A polynomial fit to the scaled data yielded

$$\psi(z) = [3.79\, z + 33.7\, z^3 - 6.64\, z^5 + 0.332\, z^7] \exp(-3.04\, z) \tag{37}$$

and the normalized moments C_q were found to be practically independent of energy (see Section 3). Slattery has taken these results as an evidence for the precocious onset of the KNO scaling in the range from 50 to 300 GeV/c. The result is quite surprising because KNO scaling prediction is based on explicitly asymptotic arguments which are not yet valid in the energy range considered. In particular, in this range the inclusive cross-sections have not yet developed a well defined rapidity plateau and $\langle n\rangle$ does not yet increase as log s.

As remarked by Slattery, the data at lower energy (19 GeV) do not follow the universal curve (37). In fact one can see from Fig. 19 that all the data in the range from 12 to 35 GeV/c seem to follow better another curve which is (1) narrower and (2) higher at the maximum (by $\sim$ 20 percent) than (37); the modes for the two sets of points are not in the same position.

The difference in width can be understood as follows. When one plots P_n as a continuous function of n (making an interpolation for non-integer n) then one gets a curve of a unit area because of the normalization condition: $\sum_n P_n \to \int P_n dn = 1$. The curves for each energy are then rescaled by multiplying the horizontal axis by $\langle n\rangle^{-1}$ and the vertical axis by $\langle n\rangle$, so that the normalization is maintained. Thus if the width of each curve, or D, is proportional to $\langle n\rangle$, *i.e.* $D/\langle n\rangle = \text{const.}$, the scaled curves will all have the same width. But we know already from Section 3 that the condition $D/\langle n\rangle = \text{const.}$ is approached slowly because $D/(\langle n\rangle - 1) = \text{const.}$ When we use instead of z another scaling variable $z' = (n-1)/(\langle n\rangle - 1)$ and plot $P_n(\langle n\rangle - 1)$ *vs* z', we find indeed that all the points in the 12–303 GeV/c range follow better a single curve (Fig. 20), although the differences in the position of the mode are still present.

Now, the position of the mode provides a sensitive test for semi-inclusive scaling. The average value of $\psi(z)$ is, by definition, at $z = 1$. For the rescaled curves to have similar shape it is then necessary that

$$\frac{M_0}{\langle n\rangle} = z_0 = \text{const.} \tag{38}$$

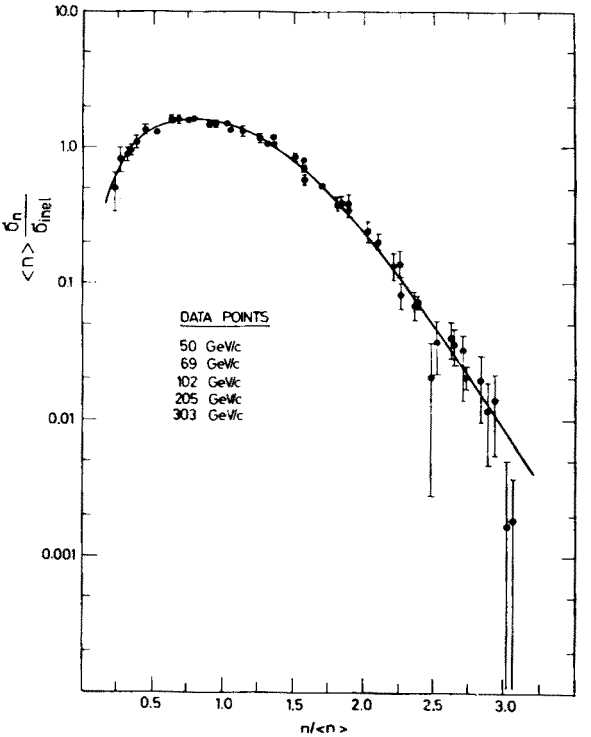

Fig. 18. Slattery's plot of $\langle n \rangle P_n$ *vs* $z = n/\langle n \rangle$ (from Ref. [4]). The curve is a polynomial fit to the data

Fig. 19. Plot of $\langle n \rangle P_n$ *vs* $z = n/\langle n \rangle$ for data at 12–24 GeV/*c* (full circles), 28–35 GeV/*c* (crosses), 50 GeV/*c* (triangles) and 69–303 GeV/*c* (open circles)

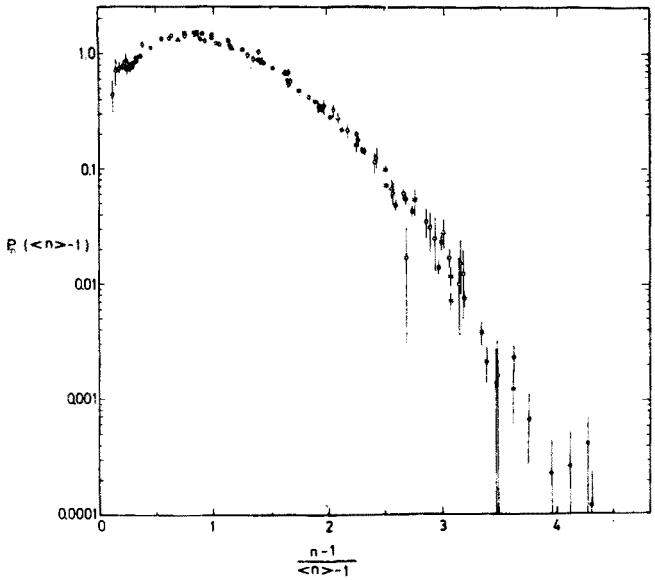

Fig. 20. Plot of $(\langle n\rangle - 1)P_n$ *vs* $z' = (n-1)/(\langle n\rangle - 1)$ for data in the range from 12 to 303 GeV/c. Symbols are the same as in Fig. 19

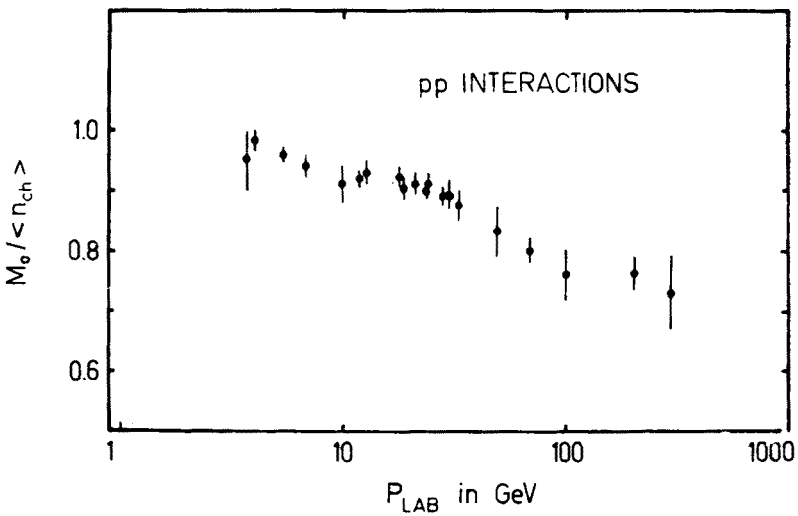

Fig. 21. The ratio $M_0/\langle n\rangle$ for pp collisions

However Fig. 21 shows that the ratio in question changes smoothly in the whole energy range considered and it does not seem yet to approach a plateau. Using Slattery's fit (37) Schlitt [13] has computed $z_0 = 0.8$ and $\psi(z_0) = 1.6$ for the "universal" curve in the 50 to 303 GeV/c range. It can be seen from Fig. 21 that Schlitt's value gives indeed an average position of $M_0/\langle n\rangle$ for the considered energy range but the physical meaning of this result is doubtful.

If one assumes that the ratio $M_0/\langle n\rangle$ is approaching a limiting value as $1/\langle n\rangle^2$ one can get a good fit to data giving $\lim_{s\to\infty} M_0/\langle n\rangle = 0.6$ which is still rather far from what we find in the range from 50 to 303 GeV/c.

The question of an early KNO scaling has been also investigated by Fiałkowski and Miettinen [14], who have studied several "reasonable" theoretical models. In these models the approach to the asymptotic KNO scaling limit occurs extremely slowly. The authors conclude that the real KNO scaling limit (if any) may be very different from that deduced [4] from the present data.

My conclusion of this section is that there is rather weak evidence for an early semi-inclusive scaling in the 50 to 303 GeV/c range.

7. *Buras-Koba scaling (BK scaling)*

Recently Buras and Koba [15] have proposed to use a variable

$$w = \frac{\pi}{4} z^2 = \frac{\pi}{4}\left(\frac{n}{\langle n\rangle}\right)^2 \tag{39}$$

to describe the normalized multiplicity distributions at high energies. The authors have introduced a new scaling function

$$\Phi(w) = \frac{1}{\pi}\frac{\langle n\rangle^2}{n} P_n = \frac{1}{\pi z}\psi(z), \tag{40}$$

where $\psi(z)$ is the KNO scaling function (see Section 6); the factors $\pi/4$ and $1/\pi$ in (39) and (40) are for normalization purpose. The pp data in the 50–303 GeV/c range fit very well to a simple function

$$\Phi(w) = \exp(-w) \tag{41}$$

which gives a straight line with unit slope in the semi-log plot of $\Phi(w)$ *vs* w (see Fig. 22). The formula (41) is directly connected to the empirical formula (31) of Bozoki *et al.* with $\beta = 2$. In order to explain this simple behaviour the authors have introduced a Local Excitation Model in which the hadron-hadron collision is imagined as consisting of collisions between a number of constituents of one hadron and those of the other. The details of the model are given in Ref. [16].

The Buras-Koba conjecture of an early semi-inclusive scaling (BK scaling) is open to the same criticism as Slattery's observation on the early KNO scaling (see Section 6). When one plots the lower energy data from the 12–28 GeV/c range using BK variables one finds large deviations from (41). The points for two prongs and the high multiplicity tail lie below the straight line given by (41), whereas the points for four prongs are above it (see Fig. 23). This would suggest that different multiplicities approach the limiting distribution (41) in a different way.

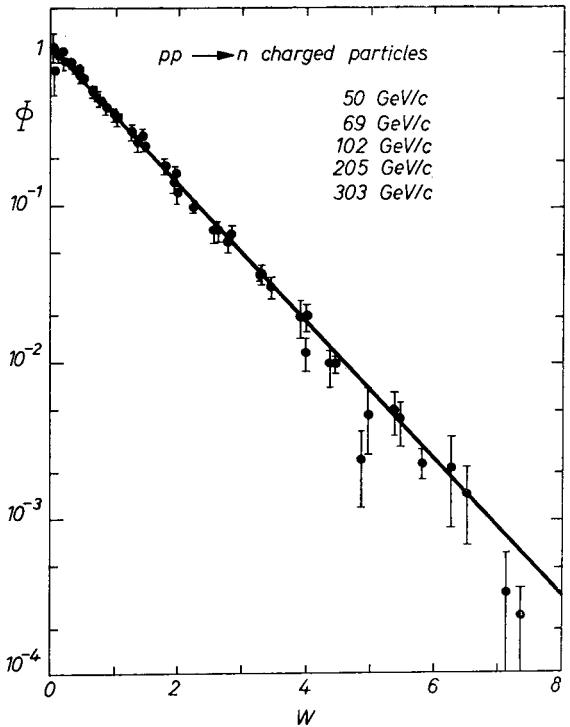

Fig. 22. Buras-Koba plot for pp collisions in the range from 50 to 303 GeV/c (from Ref. [15])

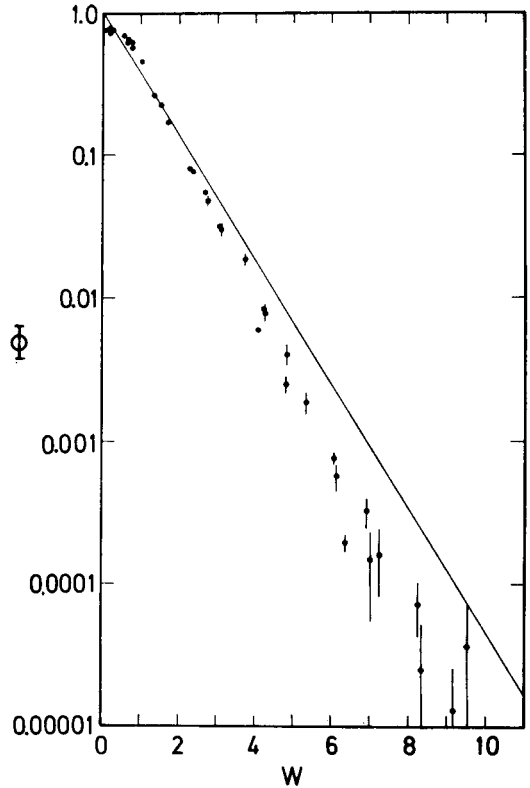

Fig. 23. Buras-Koba plot for pp collisions in the range from 12 to 28 GeV/c. The straight line represents $\Phi(w) = \exp(-w)$ as in Fig. 22

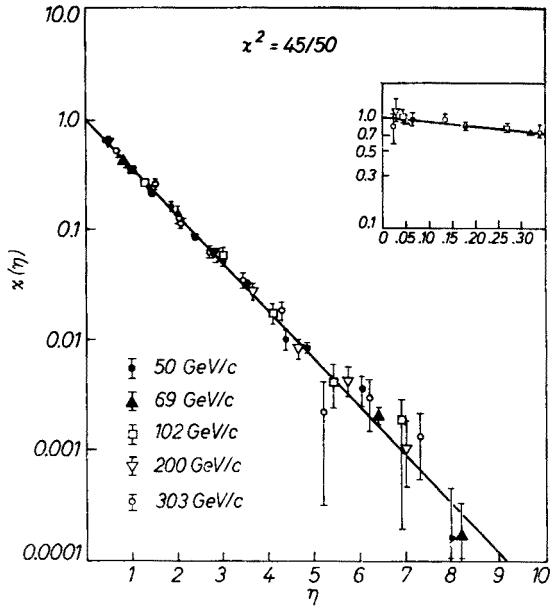

Fig. 24. Rama Rəo-Sarma plot for pp collisions in the range from 50 to 303 GeV/c (from Ref. [17])

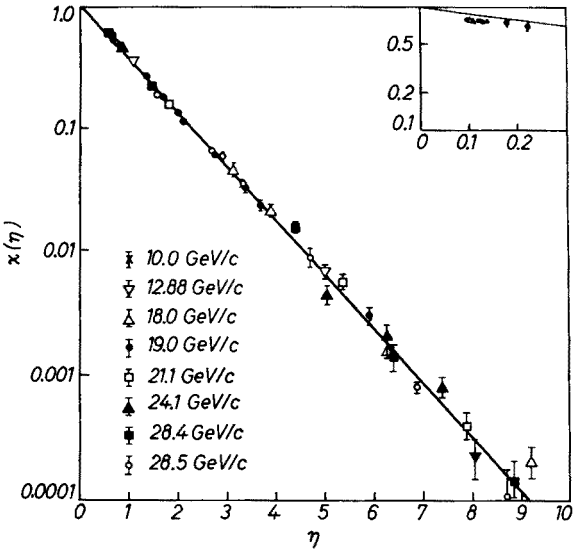

Fig. 25. Rama Rao-Sarma plot for pp collisions in the range from 10 to 28.5 GeV/c (from Ref. [17]). The insert shows details of the plot for small η (two-prong events). The straight line in this and preceding figure represents the exponential given by formula (43)

Rama Rao and Sarma [17] pointed out recently that the available data for pp collisions scale better in terms of a new variable

$$\eta = \frac{n(n-1)}{\langle n(n-1)\rangle} \tag{42}$$

which being proportional to the number of pairs of charged particles may provide a better insight into the mechanism of production process. The new scaling function

$$\chi(\eta) = \frac{1}{2} \cdot \frac{\langle n^2-n\rangle}{2n-1} P_n = \exp(-\eta) \tag{43}$$

gives indeed rather good representation of data in both lower and higher energy range (see Figs 24 and 25). One may notice, however, that the points for two prongs in lower energy range lie systematically below the straight line (43) as in the case of the BK scaling.

My own modification of the Buras-Koba scaling is explained in the following section.

8. Two-component model fits

During the last years a large variety of models has been proposed in order to explain general features of inelastic collisions of particles at high energy. The observed features of topologic cross-sections have ruled out many of these models as only mechanisms of particle production. For example, an essential feature of diffraction models is that the topologic cross-sections eventually become independent of energy, for which there is yet no evidence even at lowest multiplicities. On the other hand, the fact that above 50 GeV/c the multiplicity distribution becomes broader than a Poisson distribution is rather difficult to explain using a short range correlation model (of multiperipheral type).

Many authors [18–24] have pointed out that the features of multiplicity distributions can be explained in terms of the Two-Component Model first proposed by Wilson [25]. In this model it is assumed that there exist two different mechanisms of particle production: (*i*) diffractive dissociation producing mostly low multiplicities and (*ii*) a non-diffractive production of particles ("pionization"), for which there is plenty of models (*e.g.* multiperipheral or thermodynamic model).

The two-component model approach provides an excellent fit to the multiplicity distribution below 303 GeV/c and allows also for an extrapolation to higher energies.

I shall first discuss the paper by Van Hove [19], who has shown that the linear relation (11) can be simply understood if there are indeed two distinct classes of inelastic collisions. Let us denote by p_1 and $p_2 = 1-p_1$ the probabilities for an inelastic collision to belong to the components 1 and 2. Let $\langle n_i\rangle$ and D_i be the average multiplicity and the dispersion for component i:

$$D_i^2 = \langle n_i^2\rangle - \langle n_i\rangle^2, \tag{44}$$

where $i = 1,2$. We have then

$$\begin{aligned} \langle n\rangle &= p_1\langle n_1\rangle + p_2\langle n_2\rangle, \\ \langle n^2\rangle &= p_1\langle n_1^2\rangle + p_2\langle n_2^2\rangle. \end{aligned} \tag{45}$$

Using (44) and (45) it is easy to show that the dispersion D for the full set of inelastic collisions is given by

$$D^2 = \langle n^2 \rangle - \langle n \rangle^2 = p_1 D_1^2 + p_2 D_2^2 + p_1 p_2 (\langle n_1 \rangle - \langle n_2 \rangle)^2. \tag{46}$$

For $\langle n_1 \rangle \gg \langle n_2 \rangle$ we obtain

$$D \approx A \langle n \rangle - B,$$

where

$$A = (p_2/p_1)^{1/2},$$

$$B = A\langle n_2 \rangle - \frac{p_1 D_1^2 + p_2 D_2^2}{2A\langle n \rangle}. \tag{47}$$

Experimentally, the slope A is constant in the range from 4 to 303 GeV/c (see Section 3). This means that the p_i are constant. Using (11a) one finds $p_1 \approx 3/4$, $p_2 \approx 1/4$ for pp collisions. For πp collisions in the range from 4 to 25 GeV/c the slope $A = 0.44$ [3] which gives $p_2 \approx 0.16$. However, recent data at 50 GeV/c [26] and 205 GeV/c [27] for π^-p interactions show the slope A close to the value found for pp collisions (see Fig. 26).

As an example of the two-component model fit to the multiplicity distribution I shall discuss the paper of Fiałkowski and Miettinen [20]. They have assumed that the ratio of the two components is energy independent. For the non-diffractive part the simplest choice of independent emission of pairs of secondary particles was assumed. This leads to a Poisson distribution in multiplicity of negative pions n_- for the non-diffractive component. The $(2n_-+2)$-prong cross-section was then calculated from the formula

$$\sigma_{2n_-+2} = \sigma_\pi e^{-\langle n_- \rangle_\pi} \frac{\langle n_- \rangle_\pi^{n_-}}{n_-!} + \sigma^D_{2n_-+2}, \tag{48}$$

where σ_π is the total cross-section for non-diffractive ("pionization") component and σ^D refers to the diffractive part. The contributions $\sigma^D_{2n_-+2}$ were found to be constant in the range from 15 to 303 GeV/c for $n = 0, 1, 2, 3$ (that is for 2, 4, 6 and 8 prongs). The ratio σ^D/σ_π was found to be 0.28, what corresponds to $p_2 = 0.23$[3].

The extrapolation of this simple model to higher energies gives a very interesting prediction of a dip which should develop between the diffractive and non-diffractive components inside the ISR range (see Fig. 27). At 5000 GeV/c the two components would be already largely separated and the cross-section for 4-prongs would be about twice as large as those for 8 and 10-prongs[4]. This conjecture has however little support in the results of emulsion studies of cosmic ray jets. For example, the "world survey" sample of jets at $\sim$ 10000 GeV contains many more 10-prongs than 4 or even 6 prongs (see Fig. 2 in

[3] Other authors find similar values for the percent of diffraction. The values of p_2 are: 0.16 [21], 0.19 [23], 0.25 [22] and 0.27 [24].

[4] This prediction of a bimodal multiplicity distribution at high energies is common to all other models with energy independent diffractive component [21–24].

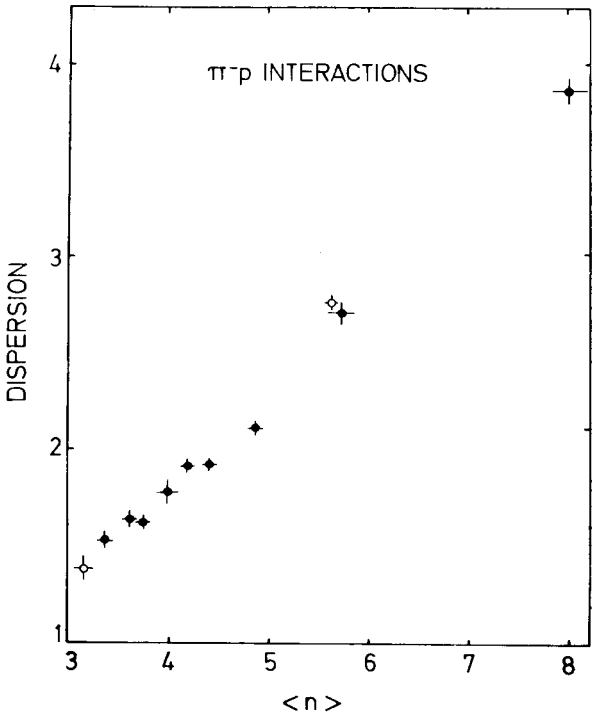

Fig. 26. Dispersion D as a function of the average charged multiplicity $\langle n \rangle$ for π^-p interactions. Empty circles show results obtained with the use of propane bubble chamber

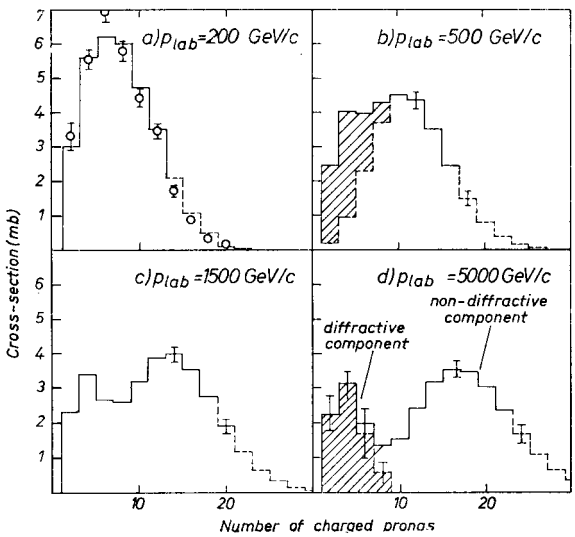

Fig. 27. The multiplicity distributions in the two-component model of Fiałkowski and Miettinen (from Ref. [20])

Ref. [28]). Because of the well known uncertainties in emulsion studies we cannot take this results for more than a hint against the model with constant diffractive component. But a good ISR experiment at 1500 GeV/c would be capable of proving or disproving this simple approach.

Finally I shall discuss my own modification of the semi-inclusive scaling in the spirit of the two-component model. As discussed before the idea of semi-inclusive scaling involves the constancy of $\langle n\rangle/D$ ratio. Experimentally we find that $(\langle n\rangle-1)/D = \text{const.}$ in

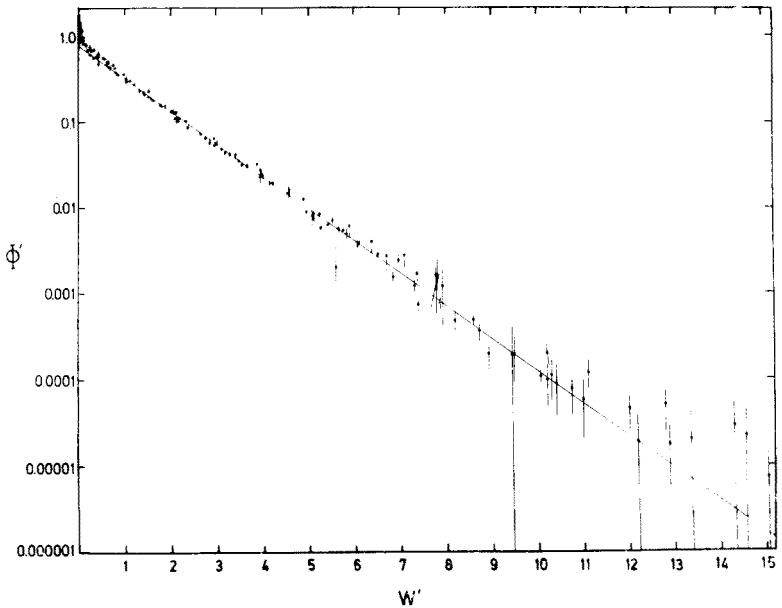

Fig. 28. The plot of Φ' *vs* w' in the modified Buras-Koba scaling. All data from Ref. [1] are included

the range from 4 to 303 GeV/c. Let us then modify the Buras-Koba variables w and Φ by replacing n by $(n-1)$. We have therefore

$$w' = \frac{\pi}{4}\left(\frac{n-1}{\langle n\rangle-1}\right)^2,$$

$$\Phi' = \frac{1}{\pi}\,\frac{(\langle n\rangle-1)^2}{n-1}\,P_n. \tag{49}$$

Fig. 28 shows a semi-log plot of Φ' *vs* w'. More than 130 data points at 21 momenta between 3.7 and 303 GeV/c are used. The straight line fit

$$\Phi' = A\exp(-Bw') \tag{50}$$

gives a very good description of data for $w' \gtrsim 1$. For $w' \lesssim 1$ experimental values lie mostly

above the line (fitted for $w' > 1$). Fig. 29 shows the deviations of data points from the straight line separately for the five lowest multiplicities. It is seen that the "second component" is concentrated at 2 and 4 prongs and only for $p_{LAB} \gtrsim 70$ GeV begins to show up in 6 prongs. Fig. 30 gives the sum of all deviations from Fig. 29. The total cross-section for the second component increases rapidly at low incoming momenta and then levels off at ~ 4.5 mb (*i. e.* 15% of inelastic cross-section) above 20 GeV. In other words, the empirical formula

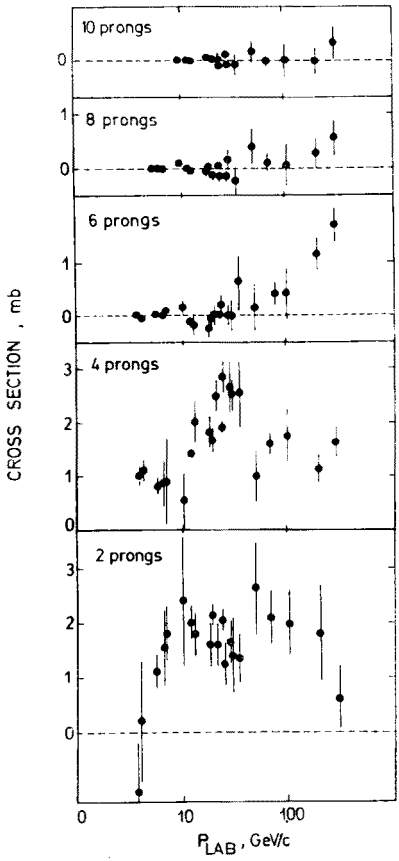

Fig. 29. The deviations of experimental points from the straight line fit shown in Fig. 28. The deviations for higher multiplicities (not shown) are very small and do not show any systematic behaviour (as in the case of 10 prongs)

(50) with two constant parameters $A = 0.78$ and $B = 0.86$ can account for about 85% of the total inelastic cross-section.

I have of course no proof that the purely empirical formula (50) describes the non-diffractive component and that the second component as given in Figs 29 and 30 represents the diffractive part of inelastic pp collisions. However the second component as found with the use of formula (50) fits exactly in the place in which we do expect the diffraction part. One may notice also that in this approach the second component contribution to each

multiplicity is no longer fixed constant although its total cross-section is obtained to be roughly constant. The unlikely bimodality of the multiplicity distribution at higher energies may thus be avoided.

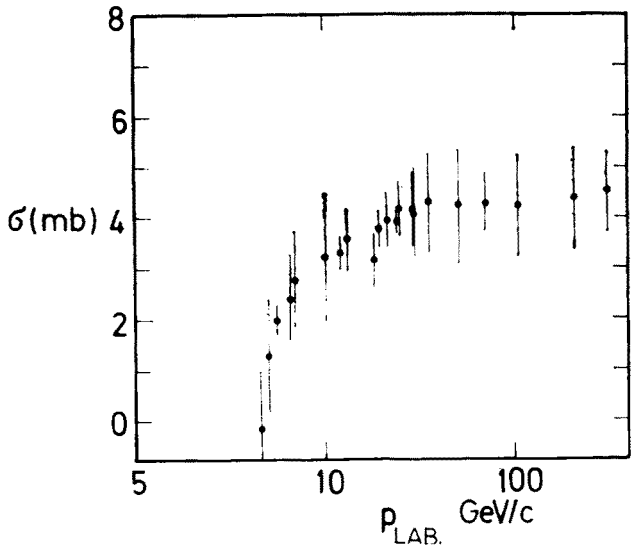

Fig. 30. The total cross-section for the second component as a function of laboratory momentum

9. *Conclusions*

1. The study of charged multiplicity distributions in pp collisions has revealed important empirical regularities.

2. There is rather weak experimental evidence for an early onset of KNO semi-inclusive scaling below 300 GeV/c. Present energies are probably still far from the Asymptopia. As remarked by Giacomelli: "The asymptotic region would seem to be round the corner, but this conclusion was already reached at previous conferences and therefore cannot be taken too seriously" [29].

3. The two-component models provide excellent fits to the multiplicity distribution. The diffractive component is found to be between 15 and 30 percent of the total inelastic cross-section. The bimodality of multiplicity distributions predicted by many models for energies above 1000 GeV has to be investigated by ISR experiments.

REFERENCES

[1] G. A. Smith *et al.*, *Phys. Rev.*, **123**, 2160 (1961); E. L. Hart *et al.*, *Phys. Rev.*, **126**, 747 (1962), (3.67 GeV/c).
L. Bodini *et al.*, *Nuovo Cimento*, **58A**, 475 (1968); S. Coletti *et al.*, *Nuovo Cimento*, **49A**, 479 (1967), (4 GeV/c).
G. Alexander *et al.*, *Phys. Rev.*, **154**, 1248 (1967), (5.5 GeV/c).
E. R. Gellert, LBL-749 (1972), (6.6 GeV/c).

G. Yekutieli *et al.*, *Nuclear Phys.*, **B18**, 301 (1970); G. Danieli *et al.*, *Nuclear Phys.*, **B27**, 157 (1971), (6.9 GeV/*c*).
S. P. Almeida *et al.*, *Phys. Rev.*, **174**, 1638 (1968), (10 GeV/*c*).
D. B. Smith, UCRL-20632 and private communication from G. Oh (12.88, 18, 21.1, 24.1, 28.4 GeV/*c*).
Bonn–Hamburg–Munich Collaboration, W. Richter, *Diplomarbeit*, München University 1972, (12, 24 GeV/*c*).
H. Bøggild *et al.*, *Nuclear Phys.*, **B27**, 285 (1971), (19 GeV/*c*).
W. H. Sims *et al.*, *Nuclear Phys.*, **B41**, 317 (1972), (28.5 GeV/*c*).
I. V. Boguslavsky *et al.*, Dubna *preprint* 1972, (35 GeV/*c*).
V. V. Ammosov *et al.*, *Phys. Letters*, **42B**, 519 (1972), (50, 69 GeV/*c*).
J. W. Chapman *et al.*, *Phys. Rev. Letters*, **29**, 1686 (1972), (102 GeV/*c*).
G. Charlton *et al.*, *Phys. Rev. Letters*, **29**, 515 (1972), (205 GeV/*c*).
F. T. Dao *et al.*, *Phys. Rev. Letters*, **29**, 1627 (1972), (303 GeV/*c*).
[2] B. R. Webber, *Phys. Letters*, **42B**, 69 (1972).
[3] A. Wróblewski, *Proceedings of the III International Colloquium on Many-Body Reactions*, Zakopane 1972, p. 140; also Warsaw University *preprint* IFD/72/2.
[4] P. Slattery, *Phys. Rev. Letters*, **29**, 1624 (1972); *Phys. Rev.*, **D7**, 2073 (1973).
[5] O. Czyżewski, K. Rybicki, Institute of Nuclear Physics *Report* No 703/Ph, Cracow 1970; *Nuclear Phys.*, **B47**, 633 (1972).
[6] T. Tati, K. Yokoyama, University of Hiroshima *preprint* RRK 72–17 (1972).
[7] H. Minakata, T. Tati, K. Yokoyama, University of Hiroshima *preprint* RRK 72–18 (1972).
[8] T. F. Hoang, *Phys. Rev.*, **D7**, 2799 (1973).
[9] G. Bozoki, E. Gombosi, M. Posch, L. Vanicsek, *Nuovo Cimento*, **64A**, 881 (1969).
[10] H. Weisberg, University of Pennsylvania *preprint* UPR-0015T (1973).
[11] G. W. Parry, P. Rotelli, ICTP Trieste *preprint* IC/73/3 (1973).
[12] Z. Koba, H. B. Nielsen, P. Olesen, *Nuclear Phys.*, **B40**, 317 (1972).
[13] D. W. Schlitt, University of Utrecht *preprint* (1973).
[14] K. Fiałkowski, H. Miettinen, Rutherford Laboratory *preprint* RPP/T/44 (1973).
[15] A. Buras, Z. Koba, *Lett. Nuovo Cimento*, **6**, 629 (1973).
[16] A. Buras, J. M. Dethlefsen, Z. Koba, Niels Bohr Institute *preprint* NBI-HE-73-6 (1973).
[17] I. Rama Rao, K. V. L. Sarma, Tata Institute *preprint* TIFR/TH/73-25 (1973) and private communication from I. Rama Rao.
[18] K. Fiałkowski, *Phys. Letters*, **41B**, 379 (1972).
[19] L. Van Hove, *Phys. Letters*, **43B**, 65 (1973).
[20] K. Fiałkowski, H. Miettinen, *Phys. Letters*, **43B**, 61 (1973).
[21] H. Harari, E. Rabinovici, *Phys. Letters*, **43B**, 49 (1973).
[22] C. Quigg, J. D. Jackson, National Accelerator Laboratory *preprint* NAL-THY-93 (1972).
[23] W. Frazer, R. Peccei, S. Pinsky, C.-I. Tan, University of California, San Diego *preprint* (1972).
[24] J. Lach, E. Malamud, *Proceedings of the XVI International Conference on High Energy Physics* (Chicago and Batavia), Vol. 1, p. 240, also National Accelerator Laboratory *preprint* NAL-77, 7200.037 (1973).
[25] K. Wilson, Cornell *preprint* CLNS-131 (1970).
[26] Soviet–French Collaboration, paper submitted to the *XVI International Conference on High Energy Physics* (Chicago and Batavia 1972).
[27] D. Bogert *et al.*, NAL-Conf-73/30-EXP (1973).
[28] P. K. Malhotra, *Nuclear Phys.*, **46**, 559 (1963).
[29] G. Giacomelli, *Rapporteur's talk at the XVI International Conference on High Energy Physics* (Chicago and Batavia 1972), Proceedings, Vol. 3, p. 219.